Supplemental Material

Potent AMA1-specific human monoclonal antibody against P. vivax Pre-erythrocytic and Blood Stages

Anna C. Winnicki [1,+], Melanie H. Dietrich [6,8,+], Lee M. Yeoh [7,9], Lenore L. Carias [1], Wanlapa Roobsoong [5], Chiara L. Drago [7,12], Alyssa N. Malachin [1], Karli R. Redinger [1], Lionel Brice Feufack-Donfack [4], Lea Baldor [4], Nicolai C. Jung [6], Olivia S. McLaine [1], Yelenna Skomorovska-Prokvolit [1], Agnes Orban [4], D. Herbert Opi [7,10,11], Jetsumon Sattabongkot [5], Wai-Hong Tham [6,8], Jean Popovici [4], James G. Beeson [7,10,11], Jürgen Bosch*[1,3], and Christopher L. King*[1,2]

* Co-senior authors

[+] Co-first authors

[1] Center for Global Health and Diseases, Department of Pathology, Case Western Reserve University School of Medicine, [2] Veterans Affairs Medical Center, Cleveland, OH, [3] InterRayBio LLC, [4] Malaria Research Unit, Institut Pasteur du Cambodge, Phnom Penh, Cambodia, [5] Mahidol Vivax Research Unit, Faculty of Tropical Medicine, Mahidol University, Bangkok, Thailand, [6] Walter and Eliza Hall Institute of Medical Research, Parkville, Victoria, Australia, [7] Burnet Institute, Melbourne, Victoria, Australia, [8] Department of Medical Biology, The University of Melbourne, Parkville, Victoria, Australia, [9] Department of Medicine, The University of Melbourne, Parkville, Victoria, Australia, [10] Department of Infectious Diseases, The University of Melbourne, Parkville, Victoria, Australia, [11] Central Clinical School and Department of Microbiology, Monash University, Clayton, Victoria, Australia. [12] Department of Microbiology, Monash University, Clayton, Victoria, Australia.

Index Supplemental

Figures:
Supplemental Figure 1 – Blocking activity of serum from Cambodian individuals
Supplemental Figure 2 – HumAb Single Cycle Kinetics
Supplemental Figure 3 - Replicates of Pf-PvAMA1 cell line inhibition
Supplemental Figure 4 – Sporozoite HC04 invasion separated CSP210/247
Supplemental Figure 5 - Surface properties of PvAMA1 and its interaction partners RON2 and humAb 826827
Supplemental Figure 6 – RON2 binding groove conservation and Sequence differences between Pv, PvPNG16, Pf, Pc, Pk, Tg
Supplemental Figure 7 – Published PvAMA1 Clinical Isolates sequence conservation

Tables:
Supplemental Table 1 – Avidity Index (AI_{50}) of PvAMA1 specific humAbs to different AMA1 constructs
Supplemental Table 2 - List of SNP and haplotypes observed in AMA1 sequences in isolates tested in response to 826827
Supplemental Table 3 – Crystallography data collection and refinement statistics
Supplemental Table 4 - Interactions PvAMA1 – Fab 826827 based on PISA

Movies:
Supplemental Movie 1: Morph between open and closed conformation of AMA1 Domain Loop 2
Supplemental Movie 2: PvAMA1 bound Fab826827 compared to RON2
Supplemental Movie 3: Polymorphisms within PvAMA1 in relation to Fab826827

Supplemental Tables & Figures

Supplemental Figure 1 – Blocking activity of serum from Cambodian individuals

Inhibition of PvRON2 binding to PvAMA1 by plasma samples from Cambodian donors. Plasma samples were tested at 1/50 dilution for the ability to inhibit binding of the PvRON2 loop to PvAMA1 in a plate-based assay. Samples were tested in duplicate. Data show mean and range; the dotted line shows 50% inhibition. PBMCs from donor C5 were selected for sorting B cells specific for PvAMA1 and subsequent MAb generation.

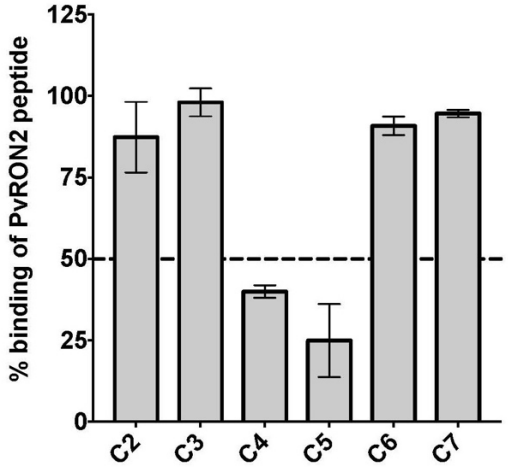

Supplement Figure 2 – HumAb Single Cycle Kinetics Curves and Results

A) Binding response curves to various concentrations of PvAMA1 for each humAb. **B)** k_{on} and k_{off} rates for each humAb determined using SPR.

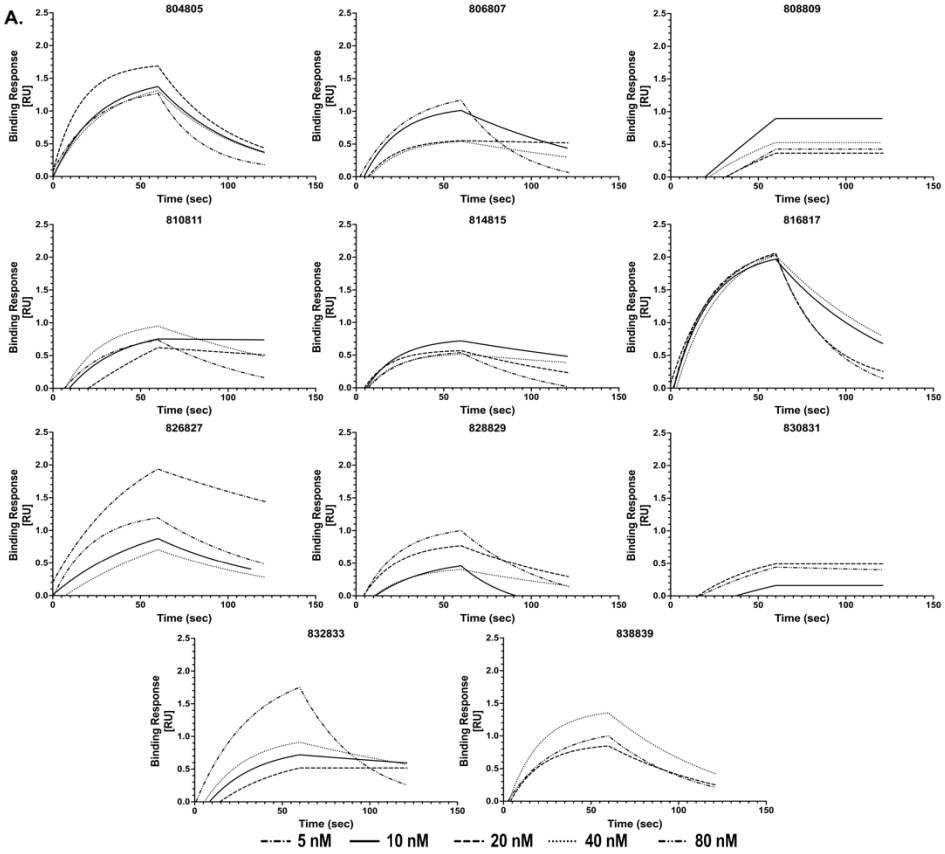

B.

	Kon	Koff
800801	0.00×10^{0}	0.00×10^{0}
804805	2.48×10^{6}	1.14×10^{-2}
806807	1.35×10^{6}	7.40×10^{-3}
808809	6.01×10^{5}	-2.35×10^{-3}
810811	8.64×10^{5}	4.44×10^{-3}
814815	2.56×10^{6}	5.30×10^{-3}
816817	1.78×10^{6}	1.46×10^{-2}
826827	6.01×10^{5}	1.02×10^{-2}
828829	1.28×10^{6}	1.32×10^{-2}
830831	1.01×10^{6}	-2.60×10^{-4}
832833	4.77×10^{5}	8.85×10^{-3}
838839	1.15×10^{6}	1.42×10^{-2}

Supplemental Figure 3 - Replicates of Pf-PvAMA1 cell line inhibition

Dose response inhibition curves of PvAMA1-specific humAbs against Pf-PvAMA1 transgenic parasites. Each humAb was tested in triplicate as indicated in different colored lines, and IC_{50} was calculated using R. 043038, an anti-tetanus toxoid humAb was used as a negative control.

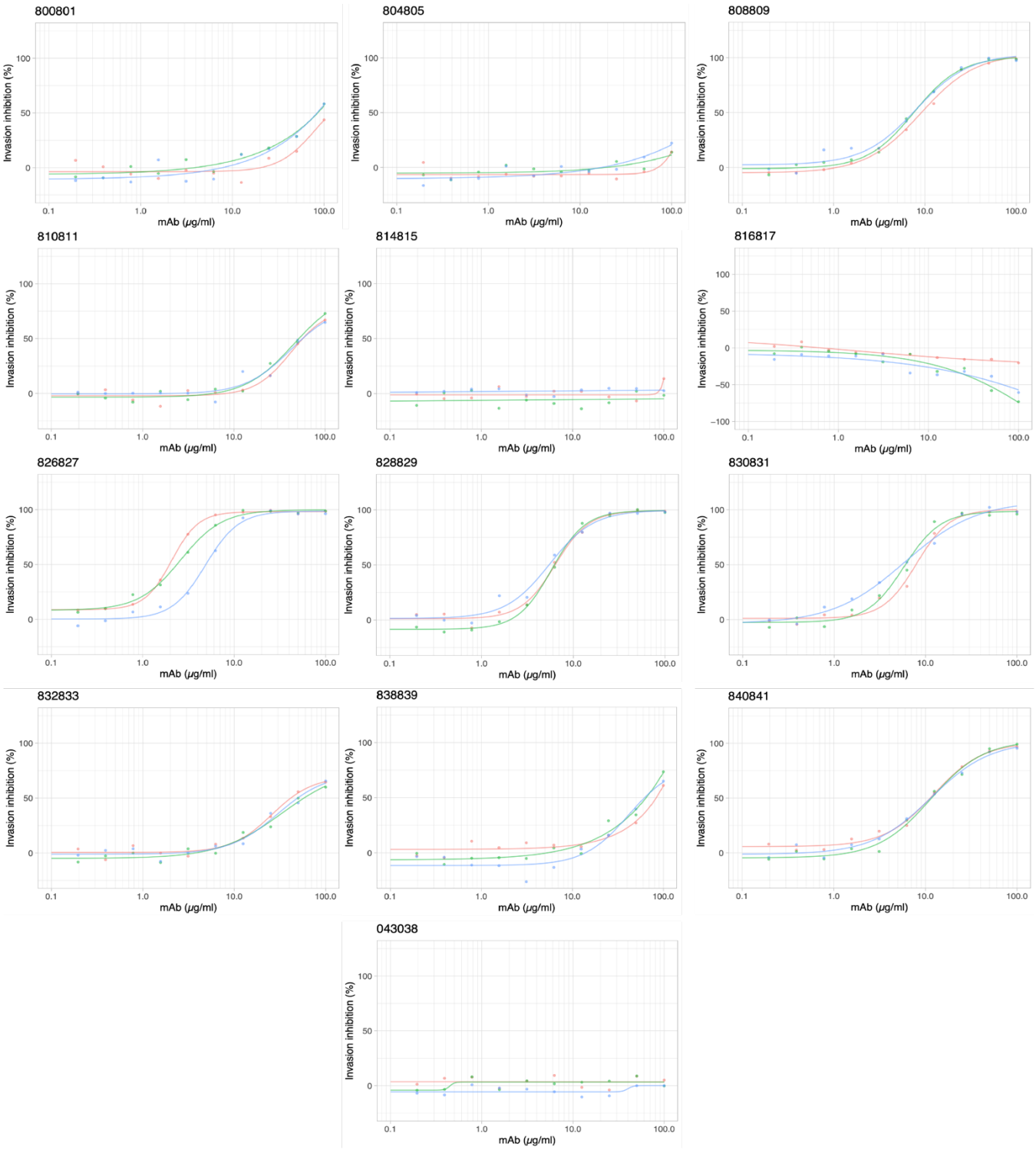

Supplemental Figure 4 – Sporozoite HC04 invasion separated CSP210/247
Dose response inhibition curves of Pv sporozoites blocking by PvAMA1 specific humAbs. Murine anti-CSP monoclonal antibodies served as positive control of blocking inhibition. Three different sporozoite isolates were used for this assay. Based on the blocking activity with the anti-CSP monoclonal one can separate two CSP210 and one CSP247 experiments. Shown

below in **A)** are the dose-responses obtained with CSP210 strains and in **B)** with strain CSP247. The calculated IC 50 for CSP210 is 0.08 µg/mL and for CSP247 IC 50 ~8 µg/mL HumAbs against PvAMA1 were randomly screened with these isolates. Of note, humAb8 26827 was screened with both sporozoite strains and shows potent inhibition in both in contrast to the CSP monoclonal.

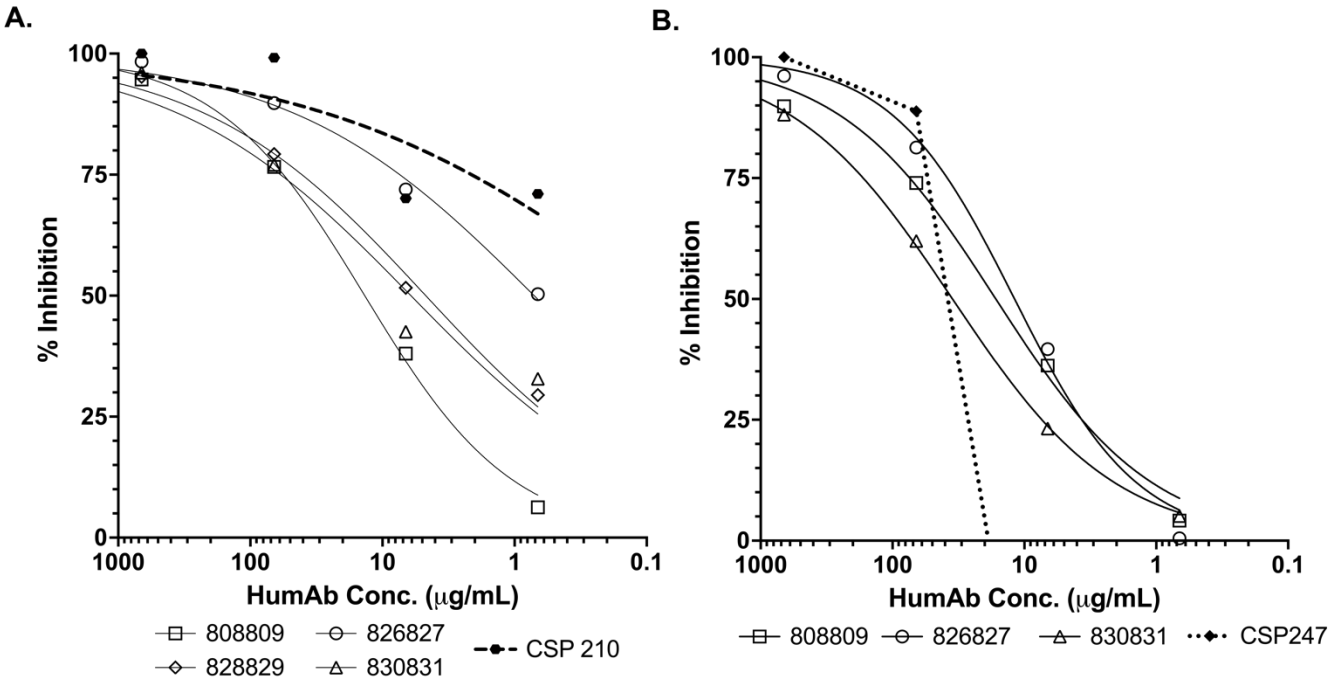

Supplemental Figure 5 - Surface properties of PvAMA1 and its interaction partners RON2 and humAb 826827

A) Schematic overview indicating the Domain 1 of PvAMA1 in gray with the Domain 2 loop in golden and the bound CDR3 loop of 826 in red. **B)** Hydrophobic surface potential of the PvAMA1 binding site. 826 was removed and rotated by 180˚ compared to the orientation in A to show the corresponding bottom interface of the interaction as well as the corresponding PvRON2 peptide. Darker areas represent higher hydrophobicity. Blue areas show hydrophilicity. **C)** Surface potential of the binding site. Red indicates negatively charged areas. Blue indicates positively charged areas. Figures were generated with Vida 4.4 from OpenEye.

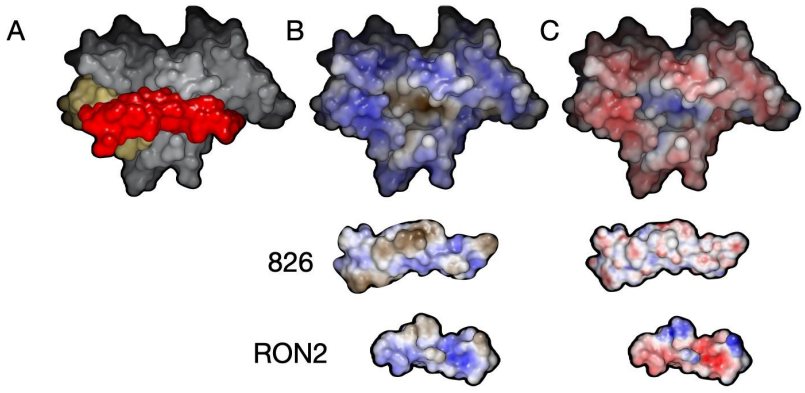

Supplemental Figure 6 – RON2 binding groove conservation and Sequence differences between Pv, PvPNG16, Pf, Pc, Pk, Tg

For all images, a residue-colored orange indicates an amino acid change between PvAMA1_PaloAlto (PDB: 8U9D) and another species' version of AMA1 **A)** Sequence conservation of residues surrounding the RON2 binding groove across 390 published clinical isolates **B)** PvAMA1_PaloAlto versus PvAMA1_PNG16 **C)** PvAMA1_PaloAlto versus *P. cynomolgi* **D)** PvAMA1_PaloAlto versus *P. knowlesi* **E)** PvAMA1_PaloAlto versus *P. falciparum* **F)** PvAMA1_PaloAlto versus *Toxoplasma gondii*.

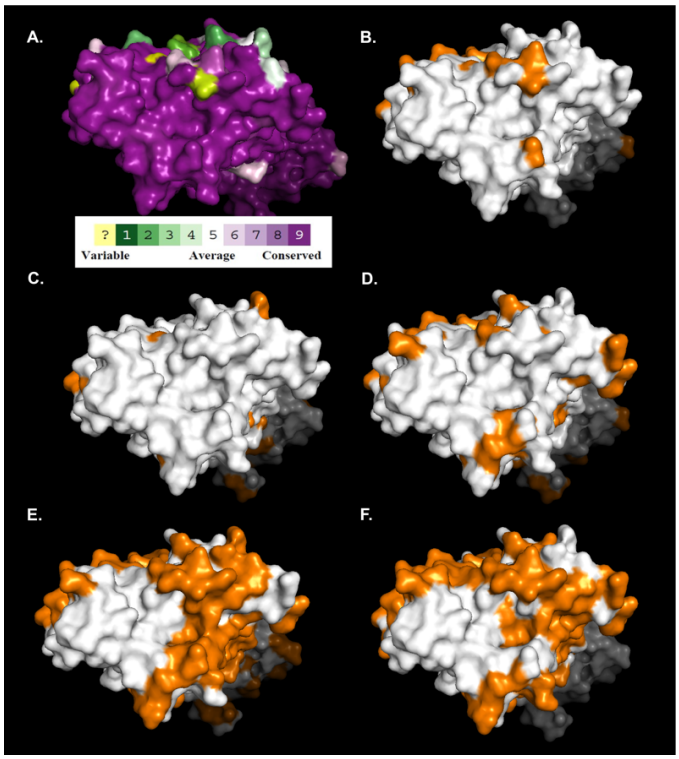

Supplemental Figure 7 – Published PvAMA1 clinical isolates sequence conservation

A) Percent conservation of each amino acid of PvAMA1 across 390 published clinical isolates. Yellow circles represent Domain 1 residues. Orange triangles represent Domain 2 residues. Blue squares represent Domain 3 residues. **B)** Percent conservation of PvAMA1 residues that contact the RON2 extracellular loop.

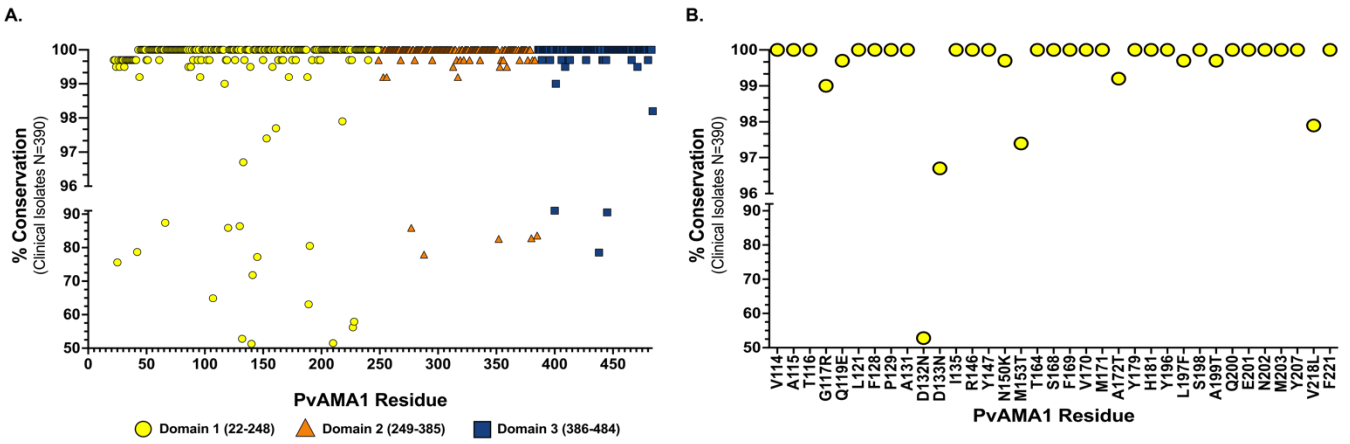

Supplemental Table 1 – Avidity Index (AI_{50}) of PvAMA1 specific humAbs to different AMA1 constructs

AI_{50}	800801	804805	806807	808809	810811	814815	816817	826827	828829	830831	832833	838839
PvAMA1_ Palo Alto	1.01	1.93	3.30	0.80	0.88	1.26	1.40	2.25	1.12	1.12	2.77	1.64
PvAMA1_ PNG16	0.96	2.57	2.93	1.04	0.87	0.76	0.93	2.08	0.78	0.53	3.00	1.43
PkAMA1	0.95	0.46	3.10	1.23	0.03	0.00	1.37	3.87	0.89	2.16	0.78	2.21

Supplemental Table 2 - List of SNP and haplotypes observed in AMA1 sequences in isolates tested in response to 826827

Haplotypes	Normalized inhibition by 826827 (100ug/ml)	D107	R112	G117	K120	N130	N132	L140	A141	E145	E189	K190	H193	P210	E227	S228	N238	V239	A276	E277	G288	K352	Q380	V382	L384	E385	R438
H1	54.34	A	TK	-	R	K	D	-	E	A	N	-	Y	S	V	D	-	-	-	K	-	-	-	-	PR	Q	H
H2	41.41	A	TK	R	R	K	D	I	-	A	NK	E	-		V	D	-	-	-	K	E	-	R	-	-	-	-
H3	51.5	A	T	-	R	-	-	-	E	A	-	-	-	-	-	-	K	L	P	K	E	-	R	-	-	-	-
H4	54.43	A	T	-	R	-	-	I	-	A	NK	E	-	-	V	D	-	-	-	K	E	-	R	E	P	-	H
H5	44.1	A	T	-	-	-	-	I	-	A	K	E	-	S	V	D	-	-	-	-	-	-	-	-	R	-	-
H6	91.3	-	K	-	R	-	-	-	-	A	-	-	-	S	-	-	-	-	-	K	E	-	-	E	P	-	H
H7	88.97	A	T	-	R	K	D	-	-	-	N	-	-	S	-	-	-	-	-	-	-	-	-	-	R	-	H

Supplemental Table 3 – Crystallography data collection and refinement statistics

	PvAMA1-Fab 826827
PDB ID	8U9D
Data collection statistics	
Wavelength (Å)	0.953725
Space group	C121
Cell axes (Å) (a, b, c)	187.24, 54.46, 104.13
Cell angles (º) (α, γ, β)	90, 97.20, 90
Resolution range (Å)	47.76-2.40 (2.54-2.40)*

Completeness (%)	99.9 (99.8)
Total no. of reflections	289692 (45358)
Unique reflections	41378 (6614)
Redundancy	7.0 (6.9)
R_{meas} (%)	18.0 (117.6)
$CC_{1/2}$ (%)	99.5 (64.2)
I/σ	9.53 (1.55)
Wilson B ($Å^2$)	42.79
Refinement statistics	
R_{work}/R_{free} (%)	19.2/ 23.5
No. of atoms	
Protein	6395
Water	259
B factors ($Å^2$)	
Chain A	46.8
Chain B	45.3
Chain C	49.6
Water	45.7
R.m.s. deviations	
Bond lengths (Å)	0.004
Bond angles (°)	0.668
Validation	
Ramachandran plot	
outliers (%)	0.0
favored (%)	96.6
Rotamer outliers (%)	0.9
C-beta outliers	0
MolProbity score	1.49

* The values in parentheses represent the highest-resolution shell.

Supplemental Table 4 - Interactions PvAMA1 – Fab 826827 based on PISA

PvAMA1	Group	826827	Location	Group	Distance
Hydrogen bonds					
Glu 83	OE2	Tyr 54	CDR-H2	OH	2.4
Glu 83	OE2	Tyr 55	CDR-H2	OH	3.3
Thr 116	OG1	Tyr 49	CDR-L2	OH	2.9
Asp 118	OD1	Gly 57	CDR-L2	N	3.0
Asp 118	OD2	Arg 54	CDR-L2	NH2	2.8
Asp 118	N	Arg 54	CDR-L2	O	2.9
Asp 118	O	Arg 54	CDR-L2	NH2	3.7
Ala 131	O	Lys 31	CDR-L1	N	2.9
Ala 131	O	Thr 32	CDR-L1	N	3.5
Asn 132	ND2	Thr 113	CDR-H3	O/N	2.8/ 3.5
Asp 133	N	Ser 30	CDR-L1	OG	2.9
Val 170	O	Cys 106	CDR-H3	N	2.7

Val 170	N	Cys 106	CDR-H3	O	2.7
Ala 172	N	Gly 104	CDR-H3	O	2.9
Tyr 196	OH	Arg 101	CDR-H3	NH2	3.5
Tyr 196	OH	Glu 103	CDR-H3	OE1/OE2	2.8/2.6
Gln 314	O	Tyr 34	CDR-H1	OH	3.6
Asn 315	ND2	Tyr 117	CDR-H3	OH	2.8
Asn 315	O	Arg 101	CDR-H3	NE	2.7
Asn 315	O	Tyr34	CDR-H1	OH	3.8
Asn 315	OD1	Arg 101	CDR-H3	NH2	3.6
Asn 316	ND2	Tyr 34	CDR-H1	OH	3.7
Lys 321	NZ	Tyr 105	CDR-H3	OH	2.6
Salt bridges					
Lys 321	NZ	Glu 103	CDR-H3	OE2	3.6
Asp 118	OD2	Arg 54	CDR-L2	NH2	2.8
Other interfacing residues in PvAMA1					
Asn 84	Gly 117	Gln 119	Phe 128	Pro 129	Asn 130
His 134	Ile 135	Arg 146	Tyr 147	Asn 150	Met 153
Thr 164	His 165	Ser 168	Phe 169	Met 171	Gly 173
Gln 175	His 181	Met 194	Gln 310	Arg 313	Arg 317
Glu 318					
Other interfacing residues in 826 (heavy chain)			Other interfacing residues in 827 (light chain)		
Ser 331	Pro 32	Gly 33	Ser 28	Ser 50	Thr 53
Tyr 35	Arg 56	Arg 99	Ala 55	Ser 56	Val 58
Gly 102	Ser 107	Phe 108	Tyr 91	Asn 92	Trp 94
Cys 111	Tyr 112	Leu 114			
Phe 115	Asp 119	Tyr 120			

Supplemental Movie 1: PvAMA1 bound Fab826827 compared to RON2
The electrostatic surface potential of PvAMA1 (8U9D) is displayed without 826827 bound to it, then the superimposed RON2 is shown in magenta followed by the 826 CD3 loop in green, showing a tight overlap in the binding site. Next the backbone of 826 and 827 are displayed to show our complete co-crystal structure.

Supplemental Movie 2: Polymorphisms within PvAMA1 in relation to Fab826827 The co-crystals structure of PvAMA1 with humAb 826827 is shown as an overview where PvAMA1 is represented as a solid surface and 826 in blue and 827 in yellow. The movie zooms towards three residues of interest namely D132, N130 and G117 which represent the wildtype amino acid residues and then these residues switch to the mutations observed in our clinical isolates as well as in the known sequences from other clinical isolates.

Supplemental Movie 3: Morph between open and closed conformation of AMA1 Domain 2 loop

A morph between PDB ID 6N87 and 8U9D is shown that focuses on the Domain 2 loop movement. The PfAMA1 structure 6N87 was superimposed onto 8U9D prior to generating the intermediate states for the moving Domain 2 loop.